IOPscience iopscience.iop.org

Home Search Collections Journals About Contact us My IOPscience

Magnetization dynamics of soft nanocrystalline thin films with random magnetocrystalline anisotropy and induced uniaxial anisotropy

This article has been downloaded from IOPscience. Please scroll down to see the full text article.

2004 J. Phys.: Condens. Matter 16 9227

(http://iopscience.iop.org/0953-8984/16/50/013)

View the table of contents for this issue, or go to the journal homepage for more

Download details:
IP Address: 129.252.86.83
The article was downloaded on 27/05/2010 at 19:28

Please note that terms and conditions apply.

INSTITUTE OF PHYSICS PUBLISHING JOURNAL OF PHYSICS: CONDENSED MATTER

J. Phys.: Condens. Matter **16** (2004) 9227–9241 PII: S0953-8984(04)84421-7

Magnetization dynamics of soft nanocrystalline thin films with random magnetocrystalline anisotropy and induced uniaxial anisotropy

C B Craus[1,4], A R Chezan[2], D O Boerma[3] and L Niesen[2]

[1] Systems and Materials for Information storage group, MESA+ Research Institute, University of Twente, PO Box 217, 7500 AE Enschede, The Netherlands
[2] Department of Applied Physics, Materials Science Centre, University of Groningen, Nijenborgh 4, 9747 AG Groningen, The Netherlands
[3] Centro de Microanalisis de Materiales (Laboratorio del Acelerador), Universidad Autonoma de Madrid, Cantoblanco, 28049 Madrid, Spain

E-mail: C.B.Craus@el.utwente.nl

Received 1 August 2004
Published 3 December 2004
Online at stacks.iop.org/JPhysCM/16/9227
doi:10.1088/0953-8984/16/50/013

Abstract

Results of frequency-dependent ferromagnetic resonance (FMR) measurements are presented for thin Fe–Zr–N nanocrystalline films with random magnetocrystalline anisotropy and induced uniaxial anisotropy. The study is done by changing the composition, the grain size and the magnitude of the induced anisotropy. We show that the magnetization dynamics is strongly influenced by the structural parameters of our samples. Although the frequency-dependent spectra can be analysed on the basis of the Landau–Lifshitz equation, an extra field H_{shift} has to be introduced in order to have agreement between the experiment and calculations. This extra field does not depend on the saturation magnetization and increases significantly when the grain size decreases from 10 to 2 nm. In addition, we observe a nonlinear decrease of the frequency linewidth with the applied dc field. After discussing various existing models we conclude that H_{shift} originates from variations in the *magnitude* of the magnetization, related with the nanocrystalline structure.

(Some figures in this article are in colour only in the electronic version.)

1. Introduction

Recently, nanocrystalline ferromagnetic materials with random orientation of the grains and induced uniaxial anisotropy were recognized as potential candidates for integration in high-frequency applications [1, 2]. In this respect, the most relevant quantity is the

[4] Author to whom correspondence should be addressed.

 © 2004 IOP Publishing Ltd Printed in the UK

frequency-dependent complex permeability, the real part of which should be sufficiently high up to GHz frequencies.

In nanocrystalline ferromagnetic materials, the magnitude of the local anisotropy field H_r determines the nature of the magnetic response of the system. When H_r is larger than the exchange field H_{ex} the spins are directed along the local anisotropy axis. In this case, although there is a small magnetic correlation length, the collective behaviour is only of minor importance. If $H_r < H_{ex}$ then the grain size, the external applied field and the induced anisotropy field will determine the collective behaviour of the system [3]. In this article we will discuss only the last category.

A small applied field or a coherent anisotropy field will be sufficient to nearly align the spins of the system. The magnetic structure is also called a ferromagnet with wandering axis (FWA). The deviation angle is correlated over a certain field-dependent length which depends on the external applied field and the magnitude of the coherent uniaxial anisotropy, if present.

As part of our structural and magnetic studies of the Fe–Zr–N system [4–6], we present here an investigation of the magnetization dynamics as a function of an external magnetic field H_{dc}, applied in the plane of the samples. The samples were oriented with the easy axis (EA) parallel or perpendicular to H_{dc}. We discuss the transversal resonance mode in relation with composition, grain size and magnitude of the induced anisotropy field of our samples.

2. Experimental setup

The samples were obtained by dc-reactive sputtering in an $Ar + N_2$ gas mixture. The targets were prepared in order to have concentration ratios between Zr and Fe of 0.01, 0.025 and 0.04. A sample holder with a controlled temperature between $-55\,^{\circ}C$ and $+220\,^{\circ}C$ was used. By controlling the temperature of the substrate we can influence structural properties like grain size and nitrogen content [7]. The sputtering power was 10 W, ensuring a deposition rate of $5\,\text{Å}\,s^{-1}$. A constant dc field of 600 Oe was applied to confine the plasma and to induce a uniaxial anisotropy.

We present in table 1 the structural parameters of the samples of this study. As expected, the grain size and nitrogen content correlate with the temperature of the substrate. When the substrate temperature was low, the grain size was small and the nitrogen content was high. Samples with larger grains and lower concentration of nitrogen were obtained at high temperatures. These effects are related to the mobility of the atomic species during deposition. Quantitative estimations of grain size and nitrogen content were done using x-ray diffraction (XRD) θ–2θ scans. The thicknesses of the samples were determined using the Rutherford back scattering (RBS) technique.

We note that the grain size is significantly smaller than the ferromagnetic correlation length ($\simeq$35 nm), so that we are in a situation that the direction of the local magnetization, averaged over an exchange-coupled volume, makes small excursions from the average direction (FWA regime).

The dc magnetic properties were investigated with a vibrating sample magnetometer (VSM). As a common feature, all samples have shown almost rectangular hysteresis loops measured in a direction parallel to the easy axis, proving that at the remanence we have a single-domain magnetic structure. The values of the coercive field were in the range of 1–10 Oe for the easy-axis orientation and 1.5–5 Oe for the hard-axis orientation.

The magnetization dynamics was studied using a copper single coil connected to a network analyser (HP8720A and HP8720S). The frequency band for which we have designed the device was from 130 MHz up to 6 GHz. By measuring the reflection parameter S11 of the single coil, the complex permeability can be obtained from an appropriate analytical description of the

Table 1. Characteristics of the sputter-deposited samples. The various columns give the Zr content, the substrate temperature T, the average grain size $\langle D\rangle$ and the layer thickness t.

Sample name	Zr (at.%)	T (°C)	$\langle D\rangle$ (nm)	t (nm)
A1	1	−30	2	50
A2	1	200	13	60
B1	2.5	−55	1	100
B2	2.5	207	11	100
C1	4	−64	2	100
C2	4	215	7	100

device [8]. A proper subtraction of the substrate signal was done by orienting the sample with the magnetization parallel to the orientation of the RF field. In this case, the magnetic response vanishes. Measurements with this technique were done with the external applied field and RF field aligned in the plane of the sample. We have also measured the FMR response in the X band (9.4 GHz) with a standard electron spin resonance (ESR) spectrometer. All experimental investigations presented in this article were performed at room temperature.

3. Frequency-dependent permeability

Here we discuss the suitability of the description given by the Landau–Lifshitz (LL) equation as a phenomenological approach. Although the equation was initially written for coherent rotations of the spins, we will show that it describes the frequency-dependent permeability of our samples fairly well. Because this equation is nonlinear, it is difficult or impossible to solve it for the general case. Using reasonable assumptions [9] for the highly permeable films we can approximate the equation by a linear one. The assumptions are: (i) the anisotropy field is small in comparison with the saturation magnetization; (ii) the RF field is small so that the tipping of the magnetization is negligible; (iii) the damping constant α is small; (iv) the film is so thin that eddy currents can be neglected; and (v) if an external dc field $H_{\rm dc}$ is applied, then its value has to be large enough so that the magnetization is parallel to it.

Neglecting the terms of order higher than α^2, the general form of the LL equation is:

$$\frac{\mathrm{d}\mathbf{M}}{\mathrm{d}t} = -\gamma(\mathbf{M}\times\mathbf{H_{eff}}) - \frac{\alpha\gamma}{\mathbf{M}}[\mathbf{M}\times(\mathbf{M}\times\mathbf{H_{eff}})], \tag{1}$$

where $\mathbf{M}$ is the magnetization and $\mathbf{H_{eff}}$ the effective field. The external RF field is taken as $\mathbf{H}_{\rm RF}(t) = \mathbf{H}_{\rm RF0}\mathrm{e}^{\mathrm{i}\omega t}$. With these considerations, we can write the magnetization and the effective field as follows:

$$\mathbf{M} = \mathbf{M_S} + m(t), \qquad \mathbf{H_{eff}} = \mathbf{H}_{\rm dc} + \mathbf{H}_{\rm RF}(t) - \mathbf{H}_{\rm dem} + \mathbf{H}_k, \tag{2}$$

where $\mathbf{H}_{\rm dem}$ is the demagnetizing field and $\mathbf{H}_k$ is the anisotropy field. The magnetization is along the OX axis and $\mathbf{H}_{\rm dem} = (0, 4\pi M_S, 0)$.

By inserting equation (2) in equation (1) we obtain the simplified expression for the component $\mu_{\rm xx}$ of the complex permeability tensor in two geometries:

(a) $\mathbf{H}_{\rm RF}\|$HA (hard axis), which is equivalent to $\mathbf{H}_{\rm dc}\|$EA (easy axis):

$$\mu_{\rm Hrf\|HA} = \frac{(4\pi M_S)^2}{(H_{\rm dc}+4\pi M_S)(H_{\rm dc}+H_K) - (\omega^2/\gamma^2) + \mathrm{i}\Gamma 4\pi M_S} + 1, \tag{3a}$$

(b) $\mathbf{H}_{\mathrm{RF}}\|\mathrm{EA}$, equivalent to $\mathbf{H}_{\mathrm{dc}}\|\mathrm{HA}$:

$$\mu_{\mathrm{Hrf}\|\mathrm{EA}} = \frac{(4\pi M_S)^2}{(4\pi M_S + H_{\mathrm{dc}} - H_K)(H_{\mathrm{dc}} - H_K) - (\omega^2/\gamma^2) + \mathrm{i}\Gamma 4\pi M_S} + 1, \tag{3b}$$

where $\Gamma = \alpha\omega/\gamma$ and $\gamma = g\mu_B/\hbar$ is the gyromagnetic ratio (μ_B is the Bohr magneton). We note that formulas (3*a*) and (3*b*) are valid only if $H_{\mathrm{dc}} < 200$ Oe, a proper assumption for our data on the frequency-dependent permeability.

All spectra can be fitted to a good agreement with equation (3); for an example, see figure 1. The resonant frequencies can be obtained from similar considerations:

$$f_{H_{\mathrm{RF}}\|\mathrm{HA}} = \frac{\gamma}{2\pi}\sqrt{(H_{\mathrm{dc}} + 4\pi M_S)(H_{\mathrm{dc}} + H_K)}, \tag{4a}$$

$$f_{H_{\mathrm{RF}}\|\mathrm{EA}} = \frac{\gamma}{2\pi}\sqrt{(H_{\mathrm{dc}} - H_K + 4\pi M_S)(H_{\mathrm{dc}} - H_K)}. \tag{4b}$$

These expressions are also valid for the ferromagnetic resonance at 9.4 GHz.

There are three major conclusions of this investigation which will be discussed in the next sections: (i) for the samples with a well-defined induced anisotropy the line shape is Lorentzian, indicating a purely relaxation-type process, (ii) the ferromagnetic resonance line position is shifted towards frequency values higher than that given by equation (4) and (iii) the phenomenological damping parameter has a pronounced nonlinear behaviour as a function of the external applied field.

4. Results

4.1. X-band ferromagnetic resonance

Before presenting our experimental results concerning the induced anisotropy field and the shift of the ferromagnetic resonance frequency, it is essential to determine the saturation magnetization. This is done from the in-plane FMR field-dependent measurements, see results in table 2. In these estimations we have taken the g factor as for pure Fe, $g = 2.1$ [10]. We could determine the g value for sample C1 (with the highest Zr concentration and nitrogen content) from the FMR with perpendicular and parallel field orientation with respect to the sample surface. For the latter geometry the resonance frequency is

$$f_\perp = \frac{\gamma}{2\pi}(H_\perp - 4\pi M_S), \tag{5}$$

where $H_\perp$ is the corresponding resonant field. The above formula is valid when the perpendicular component of the anisotropy is insignificant, like in our case.

Combining (4) and (5) we can obtain the g value independent of M_S. The result was $g = 2.051$ (± 0.003). Unfortunately, the maximum value of the field, possible to reach in our ESR set-up, has limited this type of measurement to only one sample. Because the sample C1 contained the maximum concentration of Zr, we assume that the g value for the other samples is closer to 2.10. We conclude that taking $g = 2.10$ for all samples may underestimate M_S by 5% at the maximum. Because the samples contained a high degree of imperfections like vacancies and voids, the evaluation of their volume has an uncertainty of 10%. Then the error bar as determined from VSM measurements is also 10%.

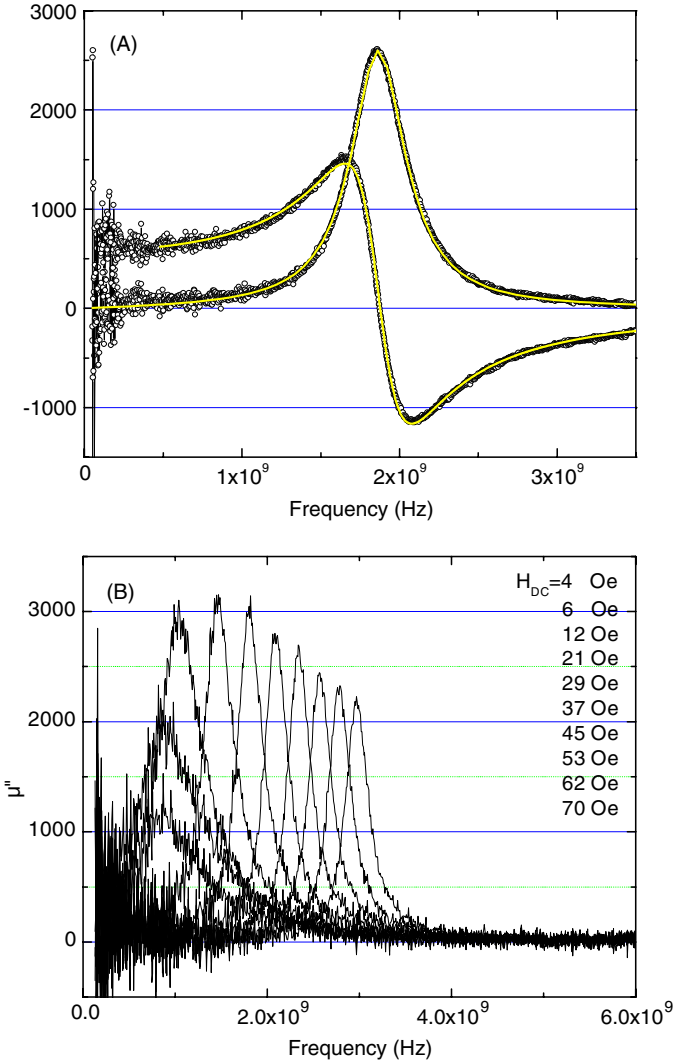

Figure 1. (A) The permeability spectra for the sample B1: ○, experimental measurement; and —, LL fit. (B) Imaginary part of the complex permeability of the sample C2; geometry $H_{RF}\|EA$. The values of H_{dc} correspond to spectra from left to right.

Table 2. Saturation magnetization $4\pi M_S$, anisotropy field as determined by frequency-dependent measurements, $H_{K\,(fr.)}$, and by X-band FMR, $H_{K\,(field)}$, and the additional field H_{shift} acting on the spins. Also average grain size $\langle D\rangle$ and nitrogen content are given.

Sample	$\langle D\rangle$ (nm)	N (at.%)	$4\pi M_S$ (kG)	H_K (fr.) (Oe)	H_K (field) (Oe)	H_{shift} (Oe)
A1	2	14	16.9	23.8 (±0.2)	25 (±2)	7.3 (±0.3)
A2	13	2	19.1	1.5 (±0.2)	0 (±2)	0 (±0.2)
B1	1	11.5	15.7	16.7 (±0.3)	18 (±2)	6.4 (±0.3)
B2	11	7	17.1	5.3 (±0.1)	9 (±2)	3.3 (±0.1)
C1	2	12	13.4	15.3 (±0.2)	13 (±2)	7.3 (±0.3)
C2	7	6	15.9	6.2 (±0.1)	7 (±2)	1.6 (±0.1)

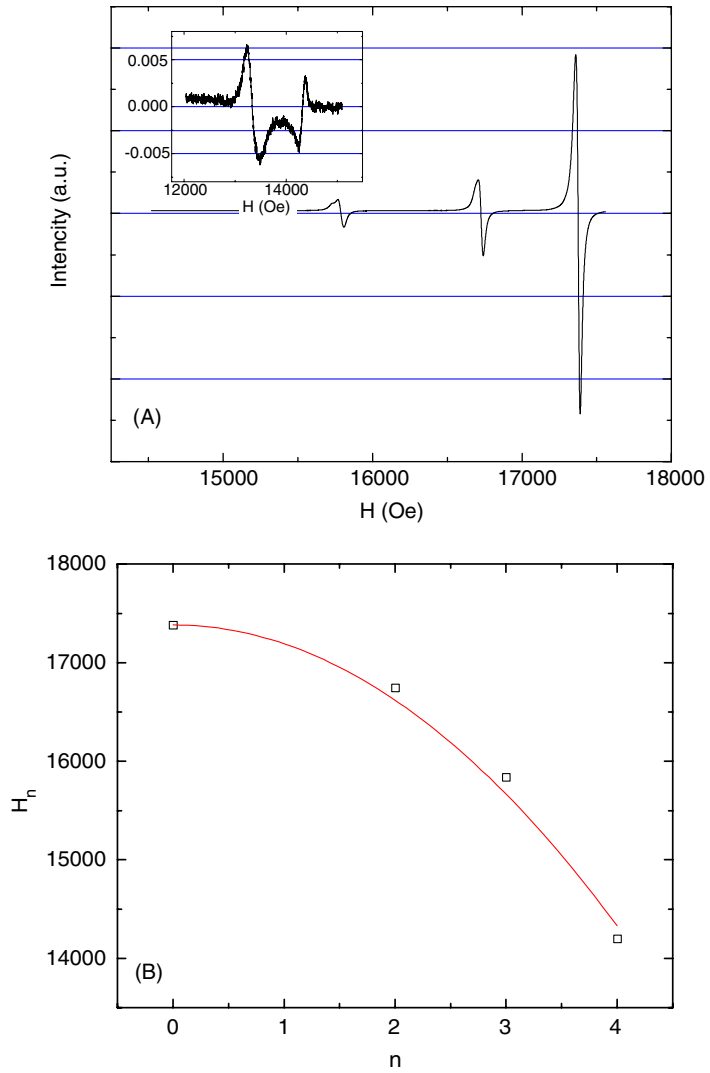

Figure 2. (A) Standing spin wave spectra for sample C1. (B) Resonance field versus resonance mode. □, experimental points; and —, simulation with the formula $H_n = H_0 - D(\pi n/t)^2$.

Standing spin waves (SSW) were excited in spectra measured in perpendicular geometry, see figure 2(A). A quadratic dependence of the line positions $H_n = H_0 - D_b(n\pi/t)^2$ on the mode number n is expected if the following conditions are met: (i) the spins are pinned to the surface, (ii) the exchange coupling constant, the internal static field and the RF field are homogenous inside the sample, (iii) the sample is saturated and there is no perpendicular component of the coherent anisotropy. D_b is called the *bulk* exchange stiffness constant of the film. For our experimental results, the closest line-indexing to a quadratic dependence is found when the second line has $n = 2$, the third line $n = 3$ and the fourth line $n = 4$. Although the resolution should be sufficient, the line corresponding to the mode number $n = 1$ was not observed. The experimental field ratios are $(H_0 - H_2)/(H_0 - H_3) = 0.41$, $(H_0 - H_2)/(H_0 - H_4) = 0.20$, $(H_0 - H_3)/(H_0 - H_4) = 0.47$ and have to be compared with

0.44, 0.25, 0.56 respectively as expected for a quadratic behaviour. A fit of D_b based on the above model leads to $D_b = 1.93\times10^{-9}$ Oe cm^2, see figure 2(B). This value can be compared with the experimental value of pure Fe [11] $D_{b\text{-Fe}} = 2.34\times10^{-9}$ Oe cm^2. We conclude that the standing wave patterns we observe cannot be described accurately by the simple model given above. The most obvious flaw of this model is the omission of the nanocrystalline structure of our material. Within the grains, the exchange constant is probably larger than that in the defected interface regions. This will lead to a complicated magnon spectrum. We note that other authors have associated the standing wave parameters with the structural correlation length [12].

4.2. Induced anisotropy field

In figure 3(A) and (B) we present the square of the FMR frequency as a function of $H_{\rm dc}$ for the samples C1 and C2. Similar data were extracted for all samples. The external field used ($H_{\rm dc} < 70$ Oe) and the anisotropy field H_K are very small compared to the saturation magnetization and consequently can be neglected in the first factor under the square root in equation (4). The slope of the graphs is consistent with the values of M_S and g calculated from the ferromagnetic resonance measurements at 9.4 GHz. Contrary to what is expected from equation (4), the lines do not cross the horizontal axis at the same distance to the origin and the FMR frequency for $H_{\rm RF}\|$EA does not reach zero value.

From the resonance conditions of both $H_{\rm RF}\|$HA and $H_{\rm RF}\|$EA, we find the dependence of H_K on the difference between the squares of the FMR frequencies:

$$H_k \cong \frac{c}{8\pi M_s}, \tag{6}$$

where $c = (f_{\rm HA}^2 - f_{\rm EA}^2)/(2\pi\gamma)^2$. HA and EA are the indices of the corresponding ferromagnetic resonance frequencies as measured for the same applied field. The values for H_K derived in this way for the samples C1 and C2 are given in figure 3(C). We see that H_K is independent of $H_{\rm dc}$, apart from the region where $H_{\rm dc}$ is close to H_K. In this case the torque on the spins is very small for the configuration 'EA' and any inhomogeneity in the sample will result in a more complicated behaviour of the local magnetization. In table 2 we present the values of H_K of all samples. These values correlate with the nitrogen concentration and with the average grain size $\langle D\rangle$. The origin of the induced anisotropy lies in the anisotropic distribution of N atoms in planes perpendicular to the external field applied during deposition [13]. Similar results for H_K were obtained from FMR measurements done by sweeping the magnetic field. However, the error bars of H_K as determined with the last-mentioned technique are comparable with the magnitude of H_K of the samples with a small nitrogen content. We conclude that the frequency sweep method is more appropriate for anisotropy field determinations.

In order to eliminate the effect of H_K on the FMR frequency, we calculate the average value $f_{\rm AV}^2 = (f_{\rm HA}^2 + f_{\rm EA}^2)/2$ for each applied field. An example for the samples C1 and C2 is shown in figure 4(A) and (B). According to equation (4), the extrapolation to zero field of the points measured above H_K, must go through the origin of the coordinate system. However, the experimental points show an evident deviation from this prediction. We can account for this difference by introducing an extra field $H_{\rm shift}$ acting on the spins, increasing the torque and the corresponding Larmor frequency. In other words, we observe an additional gap in the excitation of the uniform precession mode ($\mathbf{k} = 0$ magnon). $H_{\rm shift}$ is plotted versus $H_{\rm dc}$ in figure 4(C).

In the coherent rotation regime, where the calculated H_K is independent of $H_{\rm dc}$, we observe that $H_{\rm shift}$ is also independent of $H_{\rm dc}$. We present in table 2 the $H_{\rm shift}$ values for this regime.

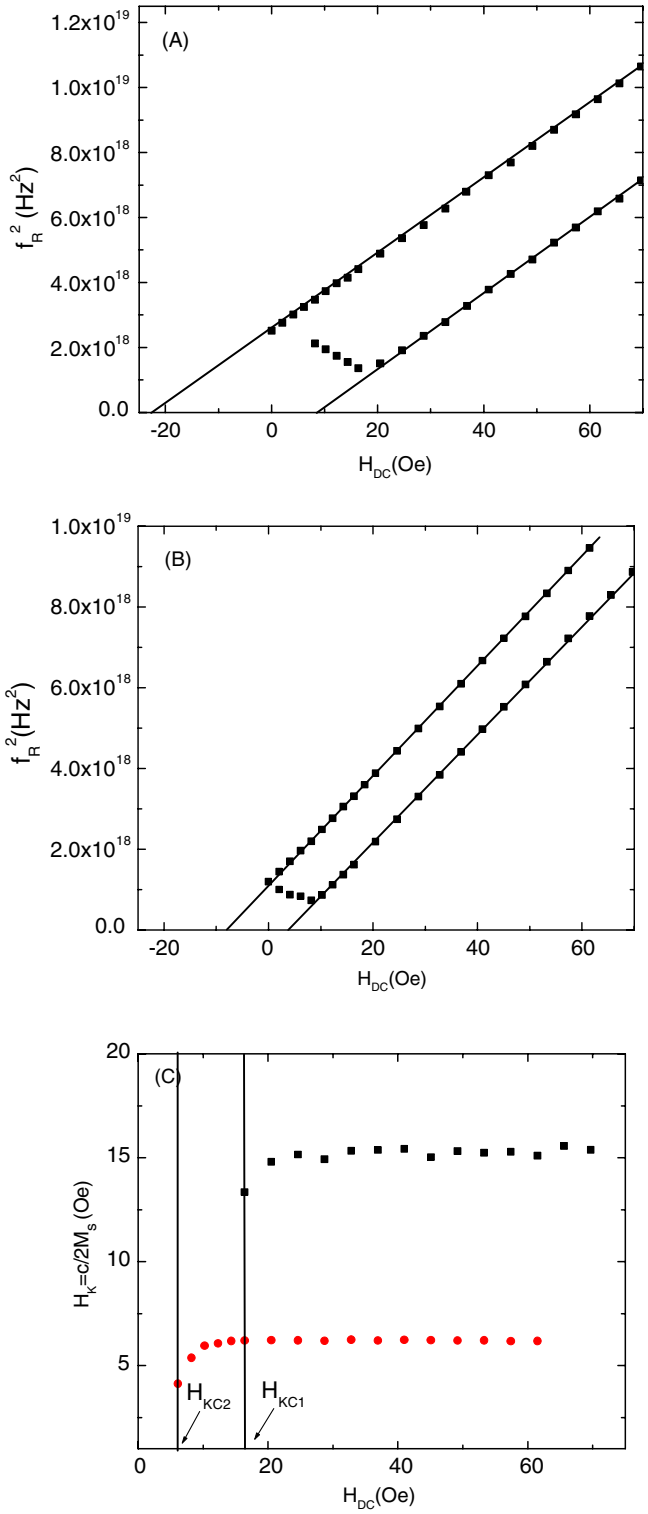

Figure 3. (A, B) The square of the resonance frequency versus H_{dc} of the samples C1 and C2. (C) Uniaxial anisotropy field of samples C1 and C2 measured in an external field from 0 to 70 Oe.

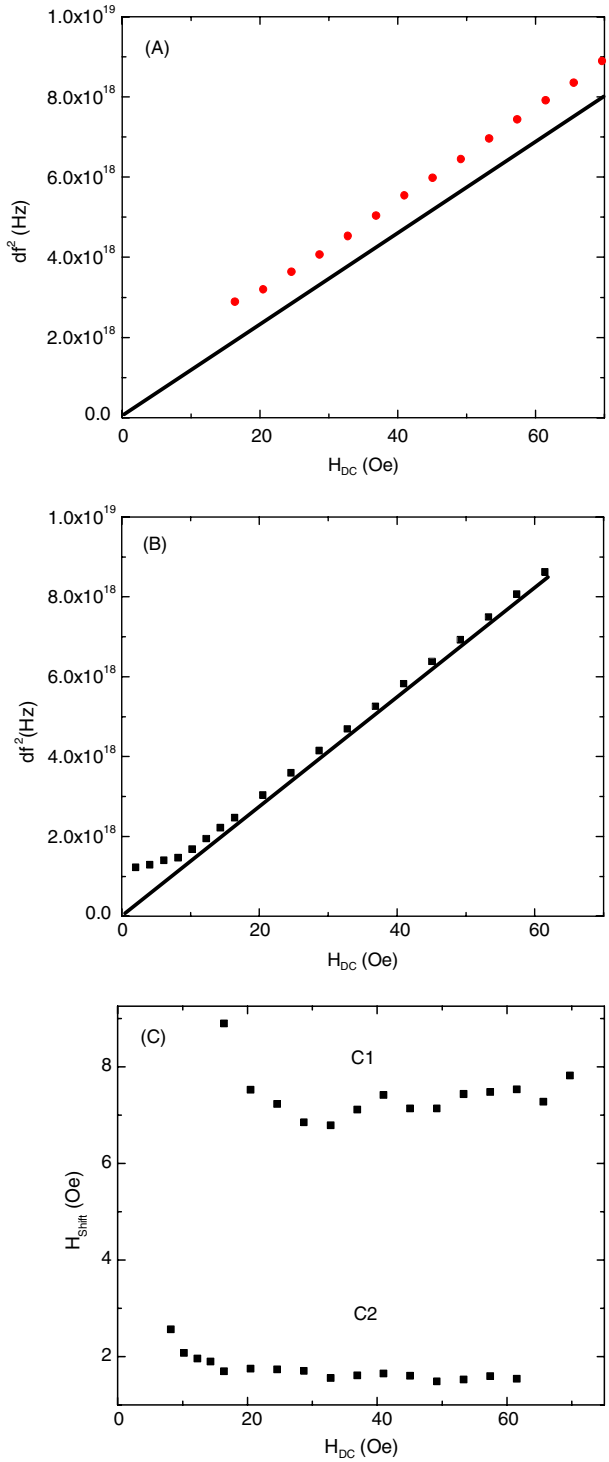

Figure 4. The average of the FMR frequencies for the sample C1 (A) and C2 (B), measured at the same external field for two geometries; (C) H_{shift} calculated from (A) and (B).

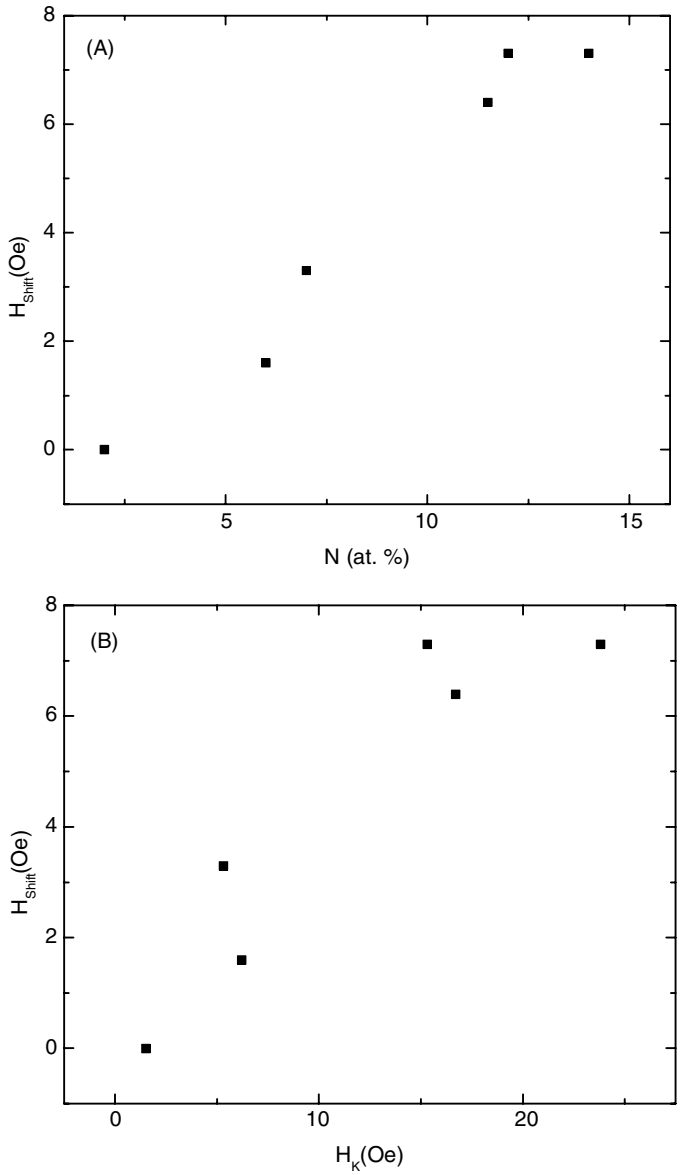

Figure 5. (A) H_{shift} versus N content and (B) H_{shift} versus H_K.

For the samples produced at low temperature, the grain size D is small, the concentration N is large, and both H_K and H_{shift} are large. For the samples made at $\sim$200 °C we have larger grains, lower nitrogen content and small values for H_K and H_{shift}. The best correlation is between nitrogen content and H_{shift}, see figure 5. On the other hand, M_S seems to have little influence on H_{shift} (compare samples A1, B1 and C1).

4.3. Line broadening

In this section we present the ferromagnetic resonance line width as a function of the external applied field. All samples showed a behaviour similar to the one in figure 6. The largest

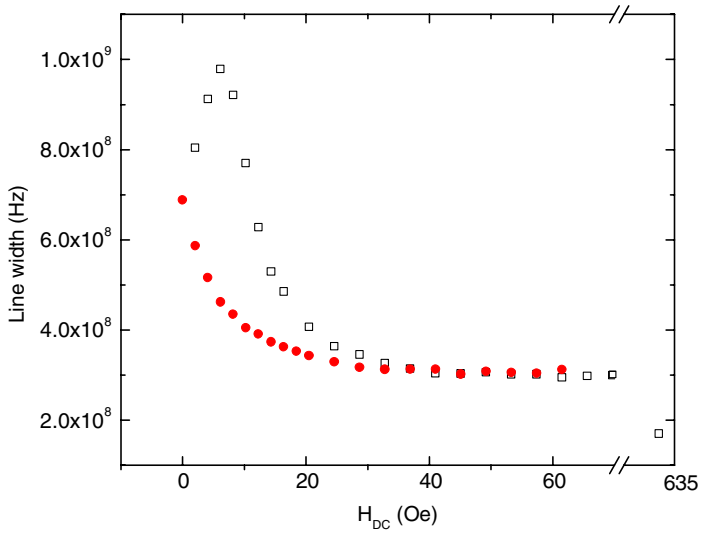

Figure 6. The FMR linewidth for sample C2 as a function of the external field, in two different geometries: □, $H_{RF}\|$EA; and ●, $H_{RF}\|$HA.

Table 3. The maximum frequency linewidth (W_{max}), the frequency linewidth measured at 60 Oe ($W_{60\,Oe}$) and the calculated frequency linewidth from the in-plane field-dependent measurements (W_{field}) versus grain size and Zr concentration.

Sample	Zr (at.%)	D (nm)	$4\pi M_S$ (kG)	W_{max} (MHz)	$W_{60\,Oe}$ (MHz)	$W_{9.4\,GHz}$ (MHz)
A1	1	2	16.9	890	460	327
A2	1	13	19.1	1160	560	380
B1	2.5	1	15.7	630	380	195
B2	2.5	11	17.1	1000	440	205
C1	4	2	13.4	580	330	160
C2	4	7	15.9	980	300	170

linewidth is observed for $H_{RF}\|$EA when the external field is almost equal to the anisotropy field. In these conditions, the resulting torque on the spins is very large suggesting an increase of the precession angle. Also the line widths are most prominent for larger grains. However, we observe that while H_{shift} becomes almost immediately constant when H_{dc} is above this region, the linewidth decreases more slowly with H_{dc}.

In order to extend this investigation to higher values of H_{dc} we present in table 3 the maximum value of the frequency linewidth, the value at 60 Oe and the value derived from the FMR measurements at 9.4 GHz. The linewidth seems to saturate at fields higher than H_K but in fact a further decrease takes place going to 9.4 GHz. This is quite different from what is observed in a classical soft material like permalloy. In that case the damping parameter α is field independent, leading to a linear but weak dependence of the linewidth on the dc field:

$$\Delta\omega = \alpha\gamma(2H_{dc} + 4\pi M_S). \tag{7}$$

A similar nonlinearity of α was observed by Sun *et al* [14] on nanocrystalline Fe–Co–N thin films.

In table 3 we can also see that the linewidth decreases with M_S. This is predicted by equation (7) if we assume that the damping parameter does not depend on M_S. Indeed, for

the last two columns of table 3 the calculated values for α do not show a correlation with M_S. Likewise, we do not observe a clear influence of the grain size on the damping parameter.

From the FMR response measured in the X-band we have calculated the frequency linewidths $\Delta\omega_{\parallel,\perp}$ of sample C1, corresponding to $H_{\rm dc}$ parallel and perpendicular to the sample surface. The values were $\Delta\omega_{\parallel}$=160 MHz and $\Delta\omega_{\perp} = 100$ MHz. The larger linewidth in the parallel case is usually associated with the presence of spin waves with energies equal to the uniform ferromagnetic resonance mode ($\mathbf{k} = 0$), enabling the so-called two-magnon process. This situation does not occur when the field is perpendicular to the sample surface [15, 16]. We will return to this point in the next section.

5. Discussion

Several effects are present in nanocrystalline films with random anisotropy that may influence the magnetization dynamics. We will discuss them here in relation with the present findings: the existence of an extra field $H_{\rm shift}$ acting on the spins and the peculiar behaviour of the FMR linewidth.

5.1. Longitudinal stray fields due to magnetization fluctuations

Hoffmann has shown [17] that fluctuations present in the FWA regime are basically one-dimensional. In a plane perpendicular to the average magnetization direction (x-axis) the spins are practically parallel, but along the x-axis the direction of the magnetization fluctuates on a length scale larger than the ferromagnetic correlation length. This gives rise to a so-called ripple pattern, which has been observed in some of our samples by Lorentz microscopy [4]. This magnetization pattern leads to magnetic charge density varying along the x-axis. Coupled to this is a stray field (demagnetizing field) directed along the x-axis. As we have shown, this stray field distribution locally influences the magnetization dynamics, giving rise to a distribution of resonance frequencies [4]. For relatively large sinusoidal magnetization fluctuations, it leads to a double hump in the FMR response. Note, however, that our treatment does not lead to an average shift of the resonance frequency.

Although we have observed these effects for samples deposited on rough substrates, where bumps and pits can lead to additional stray field distributions [18], this is not the case for the samples presented here. On the basis of the treatment given by Hoffmann [17] we estimate that effects of the stray field distribution are negligible even for the samples with relatively large grains, except possibly for the region close to H_K in the EA configuration, where the spin system is very susceptible to local inhomogeneities. In accordance with this estimate we do not see any deviation in the line shape behaviour from the simple LL behaviour (equations (3)).

5.2. Random anisotropy model

Saslow and co-workers have studied a microscopic model applicable to ferromagnetic systems with random anisotropy [19, 20]. In this model the spins are subject to various magnetic fields. Apart from a possible external field, one introduces a random anisotropy field H_r which is directly related to the local magnetocrystalline anisotropy energy, and an exchange field $H_{\rm ex}$ defined as $H_{\rm ex} = Ja^2M_S/D^2$, where J is the exchange constant, a is the interatomic distance and D the characteristic length of the structural variations (i.e. the grain size). This treatment does lead to a shift in the dispersion curve of the excitations, implying also a shift in the

ferromagnetic resonance frequency (transversal mode), for which one can write

$$H_{\text{shift}} = \frac{H_r^2}{3H_{\text{ex}}}, \tag{8}$$

i.e. H_{shift} is proportional to D^2.

Apart from the fact that numerical estimates give a small value for H_{shift}, the D-dependence is completely different from what is observed experimentally, namely H_{shift} *increases* for decreasing grain size.

Skew effect. The skew effect appears when we deal with a gradual variation in the orientation of the induced anisotropy, leading to a misalignment of the magnetization on length scales much larger than discussed before. In principle, this can lead to an extra torque described by an effective field H_{skew}. We can exclude such an effect in our samples for the following reasons: (i) no magnetic response was observed in a geometry where H_{RF} was parallel to the average magnetization (easy axis) with no external field present and (ii) the theoretical treatment of the skew effect [17] predicts $H_{\text{skew}} \sim {H_{\text{dc}}}^{-1}$, which is not observed experimentally.

5.3. Variations in the magnitude of the magnetization

Although in our fine-grained samples the variation in magnetization direction is negligible because it costs too much exchange energy, the magnitude of the local magnetization will vary, mainly because the atomic density in the intergranular region will be smaller than in the interior of the grains. This will lead to local demagnetizing fields that vary on a length scale comparable to the grain size. These fields will average out in the x-direction (parallel to the external field), but this is not the case for the z-direction (in the plane of the film). Consequently, the perpendicular magnetization component M_z is associated with a magnetostatic energy density $\langle (M_z - M_{\text{av},z})^2 \rangle$ [21]. This is similar to the term $2\pi M_y^2$ for the magnetization component perpendicular to the plane.

Adapting a simple model due to Jamet and Malozemoff [22], we assume that the magnetization and the exchange stiffness vary as a sine wave in two dimensions, i.e., $M(x,z) = M_0 + M_1 \sin(kx)\sin(kz)$ and $A(x,z) = A_0 + A_1 \sin(kx)\sin(kz)$, where $M_1 < M_0$ and $A_1 < A_0$ and k is the wave vector corresponding to the magnetization periodicity. For our case, in which the wavelength $2\pi/k$ is much smaller than the exchange length and the static magnetization lies along the z-direction, the ferromagnetic resonance condition is given by

$$\omega = \gamma[4M_0(H_{\text{static}} + H_{\text{loc}})]^{1/2}, \tag{9}$$

where $H_{\text{static}} = H_{\text{dc}} \pm H_K$ and $H_{\text{loc}} = 2\pi M_1^2/M_0 = 1/2(4\pi M_1)^2/4\pi M_0$.

We conclude that we can associate our extra field H_{shift} with the term H_{loc}. With $H_{\text{shift}} = 7$ Oe and $4\pi M_0 = 17$ kOe we arrive at $4\pi M_1 \approx 5 \times 10^2$ G, or $M_1/M_0 \approx 3\%$. Such a variation in the magnitude of **M** looks very reasonable. We further note that we can easily extend the model by assuming a distribution in the wave number k. As long as the corresponding wavelengths of the fluctuations are negligible compared to the exchange length (which is a reasonable assumption for our nanocrystalline material), the result is independent of k. The standard deviation of the magnetization distribution is then given by $\sqrt{\langle M_1^2/2 \rangle}$. The fact that we observe a bigger field shift for material with smaller grains and more nitrogen suggests that the atomic density variations between grains and intergranular region are larger in that case than for material with larger grains. This is understandable, because the volume fraction of the intergranular region is larger for smaller grains.

5.4. Spin wave excitations

The classical dispersion relation for spin waves (magnons) in a thin foil can be written as

$$\omega_k^2 = \gamma^2(H_i + Dk^2)(H_i + Dk^2 + 4\pi M_S^2 \sin^2\theta_k), \tag{10}$$

where D is the spin wave constant in frequency units and θ_k the angle between the magnetization and the propagation direction $\mathbf{k}/k$. This expression assumes a homogeneous and isotropic material, apart from the small induced anisotropy field. The effective field H_i is given by $H_i = H_{\rm dc} \pm H_K$ when the external field is in the surface plane, parallel and perpendicular to the induced easy axis. On the other hand, when the external field is perpendicular to the plane and sufficiently large to magnetize the system in that direction, we have $H_i = H_{\rm dc} - 4\pi M_S$.

If we compare these expressions with the corresponding FMR frequencies, i.e. the excitation frequencies for the $\mathbf{k} = 0$ (uniform) magnon, we deduce that for an external field in the plane of the sample the energy of the $\mathbf{k} = 0$ mode is at the top of the magnon band ($k \to 0, \theta_k = 0$) whereas for the perpendicular geometry the $\mathbf{k} = 0$ mode lies at the bottom of the magnon band. This explains the presence of a two-magnon relaxation process for the parallel geometry, in which a $k = 0$ magnon is destroyed and a magnon with the same energy, but $k \neq 0$, is created. This mechanism accounts for the larger linewidth when $\mathbf{H}_{\rm dc}$ is parallel to the sample plane compared to $\mathbf{H}_{\rm dc}$ perpendicular to the plane.

In principle, a two-magnon scattering process can also be assigned to explain the decrease in line width as a function of $H_{\rm dc}$. In this case the position of the uniform mode with respect to the magnon band will change from one field to another towards the lower branch, see [23]. We mention at this point that equation (10) has to be recalculated to include the effects determined by the nanocrystalline structure.

6. Conclusions

The magnetization dynamics of nanocrystalline ferromagnetic films of the type Fe–Zr–N have been studied as a function of an external magnetic field $H_{\rm dc}$, applied parallel as well as perpendicular to the easy axis. The grain size and concentration of Zr and N were varied by changing the deposition of parameters. The complex permeability of all samples is well described by the Landau–Lifshitz–Gilbert equation. However, apart from the torques due to the external field and the uniaxial anisotropy, the spins experience an extra torque that can be described by an additional field $H_{\rm shift}$, independent of $H_{\rm dc}$. $H_{\rm shift}$ is larger for the samples with small grains and seems to correlate with the amount of N in samples. The linewidth decreases as a function of $H_{\rm dc}$, which also deviates from the behaviour of classical soft ferromagnets (Permalloy). After discussing various models for magnetic systems with random anisotropy we conclude that the extra field is due to demagnetizing fields acting on the perpendicular component of the magnetization, as was described earlier by Jamet and Malozemoff. These fields are caused by variations of the magnitude of the magnetization related with the nanocrystalline nature of the material. The data related to the line width behaviour as a function of the field and grain size represents a solid base for further theoretical calculations for spin systems with random anisotropy.

References

[1] Wang S X, Sun N X, Yamaguchi M and Yabucami S 2000 *Nature* **407** 150
[2] Korenivski V and Dover R B 1997 *J. Appl. Phys.* **82** 5247

[3] Hellman F, Shapiro A L, Abarra E N, Robinson R A, Hjelm R P, Seeger P A, Rhyne J J and Suzuki J I 1999 *Phys. Rev.* B **59** 11408
[4] Chechenin N G, Craus C B, Chezan A R, Vystavel T, Boerma D O, De Hosson J Th M and Niesen L 2002 *IEEE Trans. Magn.* **38** 3027
[5] Chezan A R, Craus C B, Chechenin N G, Niesen L and Boerma D O 2002 *Phys. Status Solidi* a **189** 833
[6] Craus C B, Chezan A R, Siekman M H, Lodder J C, Boerma D O and Niesen L 2002 *J. Magn. Magn. Mater.* **240** 423
[7] Bobo J F, Chatbi H, Vergnat M, Hennet L, Lenoble O, Bauer Ph and Piecuch M 1995 *J. Appl. Phys.* **77** 5309
[8] Pain D, Ledieu M, Acher O, Adenot A L and Duverger F 1999 *J. Appl. Phys.* **85** 5151
[9] Huijbregtse J, Roozeboom F, Sietsma J, Donkers J, Kuiper T and van de Riet E 1998 *J. Appl. Phys.* **83** 1569
[10] Hikazumi S 1999 *Physics of Ferromagnetism* (Oxford: Oxford University Press)
[11] Grünberg D, Mayr C M, Vach W and Grimsditch M 1982 *J. Magn. Magn. Mater.* **28** 319
[12] Suran G, Naili M and Rivoire M 1990 *J. Appl. Phys.* **67** 5649
[13] van de Riet E, Klaassens W and Roozeboom F 1997 *J. Appl. Phys.* **81** 806
[14] Sun N X, Wang S X, Silva T J and Kos A 2002 *IEEE Trans. Magn.* **38** 146
[15] Cochran J F, Qiao R W and Heinrich B 1989 *Phys. Rev.* B **39** 4399
[16] Hurben M J and Patton C E 1998 *J. Appl. Phys.* **83** 4344
[17] Hoffmann H 1969 *Phys. Status Solidi* **33** 175
[18] Craus C B, Chezan A R, Boerma D O and Niesen L 2004 The influence of the surface roughness on high frequency behaviour of soft ferromagnetic thin films *J. Appl. Phys.* at press
[19] Saslow W M 1983 *Phys. Rev. Lett.* **50** 1320
[20] Saslow W M 1987 *Phys. Rev.* B **35** 3454
[21] Gargill G S and Mizoguchi T 1978 *J. Appl. Phys.* **49** 1753
[22] Jamet J P and Malozemoff A P 1978 *Phys. Rev.* B **18** 75
[23] Sparks M 1965 *Ferromagnetic Relaxation Theory* (New York: McGraw-Hill) ch 5